Non-coding RNA Research 9 (2024) 772–781

Contents lists available at ScienceDirect

Non-coding RNA Research

journal homepage: www.keaipublishing.com/en/journals/non-coding-rna-research

Crosstalk among disulfidptosis-related lncRNAs in lung adenocarcinoma reveals a correlation with immune profile and clinical prognosis

Shifeng Liu [a,*], Song Wang [a], Jian Guo [b], Congxiao Wang [a], Hao Zhang [a], Dongliang Lin [c], Yuanyong Wang [d], Xiaokun Hu [a,*]

[a] Department of Interventional Medical Center, The Affiliated Hospital of Qingdao University, Qingdao, China
[b] Department of Radiology, The Affiliated Hospital of Qingdao University, Qingdao, China
[c] Department of Pathology, The Affiliated Hospital of Qingdao University, Qingdao, China
[d] Department of Thoracic Surgery, Tangdu Hospital of Air Force Military Medical University, Xi'an, China

ARTICLE INFO

Keywords:
Lung adenocarcinoma
Disulfidptosis
Prognosis
Immunotherapy response
Drug sensitivity

ABSTRACT

Disulfidptosis refers to a specific programmed cell death process characterized by the accumulation of disulfides. It has recently been reported in several cancers. However, the impact of disulfidptosis-related long non-coding RNAs (lncRNAs) on malignant tumors has remained largely unknown. In the present work, we screened prognostic disulfidptosis-related lncRNAs and studied their effects on lung adenocarcinoma. Relevant clinical data of lung adenocarcinoma cases were retrieved from The Cancer Genome Atlas (TCGA) database. RNA sequencing was used to identify differentially expressed disulfidptosis-related lncRNAs within lung adenocarcinoma. In addition, prognostic disulfidptosis-related lncRNAs were obtained through univariate Cox regression analysis. LASSO-COX was used to construct new disulfidptosis-related lncRNA signatures. Different statistical approaches were used to validate the practicability and accuracy of the disulfidptosis-related lncRNAs signatures. Furthermore, several bioinformatic approaches were used to study relevant heterogeneities in biological processes and pathways of diverse risk groups. Reverse transcriptase-quantitative polymerase chain reaction (RT-qPCR) was conducted to analyze the expression of disulfidptosis-related lncRNAs. Finally, seven disulfidptosis-related lncRNA signatures were identified in lung adenocarcinoma cells. The prognosis prediction model constructed efficiently predicted patient survival. Subgroup analysis revealed significant differences in immune cell proportion, including T follicular helper cells and M0 macrophages. In addition, *in vitro* experimental results demonstrated significant differences in disulfidptosis-related lncRNAs. Altogether, the six disulfidptosis-related lncRNA signatures could serve as a potential prognostic biomarker for lung adenocarcinoma. Furthermore, these can be used as a prediction model in individualized immunotherapy for lung adenocarcinoma.

1. Introduction

Lung cancer has emerged as one of the most common cancers worldwide and is associated with a high mortality rate [1]. Numerous studies have been ongoing to identify the best diagnostic approach and treatment strategy [2]. Non-small cell lung cancer (NSCLC) accounts for 83% of all lung cancer cases, whereas lung adenocarcinoma (LUAD) represents the most frequent NSCLC subtype with the highest morbidity [3]. Although surgical lobectomy has remained the mainstay treatment for LUAD cases, the associated 5-year survival postoperatively is poor (10%–44%) [4]. In addition, as LUAD is always diagnosed at the metastatic or advanced stage, at which, although conventional chemotherapy, radiotherapy, and immunotherapy can be applied, insensitivity to drugs results in dismal survival [5]. Consequently, the need of the hour is to identify a prognosis prediction signature to effectively and reliably predict LUAD. This will assist in the early diagnosis of LUAD, resulting in its timely treatment to obtain optimal therapeutic outcomes.

Researchers have reported that cells can undergo accidental cell death (ACD) and regulatory cell death (RCD) [6]. Apoptosis is related to several pathophysiological events, such as *in vivo* stabilization and tumor development [7]. Recently, numerous RCD modalities, such as necroptosis, apoptosis, ferroptosis, cuproptosis, cytoplasmic division,

* Corresponding authors. Department of Interventional Medical Center, the Affiliated Hospital of Qingdao University, No. 1677 Wutaishan Road, Shandong, 266000, Qingdao, China.
E-mail addresses: liushifeng0901@126.com (S. Liu), huxiaokun770@163.com (X. Hu).

https://doi.org/10.1016/j.ncrna.2024.03.006
Received 17 December 2023; Received in revised form 8 March 2024; Accepted 13 March 2024
Available online 20 March 2024

Table 1
The lists of 10 disulfidptosis-related mRNAs.

ID	Gene Name
OXSM	3-oxoacyl-ACP synthase, mitochondrial
NDUFS1	NADH:ubiquinone oxidoreductase core subunit S1
NDUFA11	NADH:ubiquinone oxidoreductase subunit A11
NCKAP1	NCK associated protein 1
NUBPL	NUBP iron-sulfur cluster assembly factor, mitochondrial
GYS1	glycogen synthase 1
LRPPRC	leucine rich pentatricopeptide repeat containing
RPN1	ribophorin I
SLC3A2	solute carrier family 3 member 2
SLC7A11	solute carrier family 7 member 11

Table 2
The lists of 10 disulfidptosis-related lncRNAs.

ID	Gene Name
ABCC6P2	ATP binding cassette subfamily C member 6 pseudogene 2 (ABCC6P2)
EMSLR	E2F1 mRNA stabilizing lncRNA (EMSLR)
LINC00987	long intergenic non-protein coding RNA 987 (LINC00987)
LINC01842	long intergenic non-protein coding RNA 1842 (LINC01842)
LINC02709	long intergenic non-protein coding RNA 2709 (LINC02709)
POLH-AS1	POLH antisense RNA 1(POLH-AS1)
SSR4P1	signal sequence receptor subunit 4 pseudogene 1(SSR4P1)
SVIL-AS1	SVIL antisense RNA 1(SVIL-AS1)
ZFPM2-AS1	ZFPM2 antisense RNA 1 (ZFPM2-AS1)
LINC00847	long intergenic non-protein coding RNA 847 (LINC00847)

immunogenic cell death, autophagy-dependent cell death, lysosome-dependent cell death, basal prolapse, reticulocyte death, and endogenous cell death, have attracted wide clinical attention [8,9]. Cancer cell apoptosis can be an effective strategy to target cell growth and survival pathways in the tumor microenvironment (TME) [10]. For instance, cell death inhibitor receptor-interacting protein kinase 1 (RIPK1) has been reported to inhibit colorectal cancer, whereas its down-regulation has been known to reduce overall survival (OS) [11]. Ferroptosis can activate immune cells within tumors through the delivery of chemotactic signals; for example, ferroptosis inducers can inhibit anticancer immunotherapy [12]. Liu et al. reported a novel cell death type recently, namely, disulfidptosis [13]. They reported that excess intracellular cystine accumulation-induced disulfide stress induces rapid cell death. It has been demonstrated that the accumulation of disulfide material in glucose-deficient tumor cells with SLC7A11 upregulation disrupts disulfide bonding across cytoskeletal proteins, causing histone skeleton collapse and cell death. However, the effect of disulfidptosis in LUAD remains unknown.

In the present work, we constructed a risk score of disulfidptosis-related lncRNAs to predict patient survival and guide clinical treatment. Disulfidptosis-related lncRNAs were related to immune infiltration and survival. Next, differentially expressed genes (DEGs) were identified to construct the risk score, which well predicted immune infiltration, patient survival, immunotherapeutic response, and tumor mutation compliance. This work illustrated that disulfidptosis-related lncRNA patterns can efficiently predict LUAD prognostic outcome, immune infiltration, as well as immunotherapeutic response. In all, our results provide novel insights into the immunotherapy of patients with LUAD.

2. Materials and methods

2.1. Datasets and patients

Clinical data and gene expression data were obtained from three LUAD datasets from The Cancer Genome Atlas (TCGA) database. In total, data from 535 LUAD cases were included.

2.2. Disulfidptosis-related lncRNA detection

In line with the results of the previous study, Additional Table 1 lists the disulfidptosis-related mRNAs [13]. First, mRNA and lncRNA expression pattern data were collected from TCGA. Next, disulfidptosis-related lncRNA expression patterns were obtained using co-expression analysis [14]. *R* was used to study the relationship of lncRNA expression with disulfidptosis-related mRNA levels in LUAD samples. Pearson's correlation coefficients were calculated to analyze the relation ($P < 0.05$; $r > 0.40$).

2.3. Risk score verification

The frequently adopted R package limma was used to analyze differentially expressed disulfidptosis-related lncRNAs and absolute log2 (fold change) > 1 and $P < 0.05$ criteria [4]. The endpoint of the study was OS. A disulfidptosis-related lncRNA model was established by univariate Cox regression analysis. A significant effect was obtained for hazard ratio (HR) > 1.

Next, the relationship between differentially expressed lncRNAs (DElncs) and prognostic outcome was analyzed. LASSO Cox regression analysis was conducted to assess the suitability of DElncs in predicting the prognosis using the glmnet R package. The expression of key lncRNAs was measured, which along with LASSO regression coefficients, was used to determine the risk score [15]. Finally, we enrolled LUAD samples into the training cohort and categorized them into high- and low-risk groups for later analysis, with the median risk score set as the threshold.

The power of our constructed prognosis prediction model was assessed by "survival" and SurvivalROC R packages [16]. In addition, the Kaplan–Meier log-rank test and "survival" package were used to evaluate the survival between the two risk groups.

2.4. Prognosis analysis and nomogram establishment

We next checked if the disulfidptosis-related lncRNA model was independent of different clinical factors, such as age, gender, clinical stage, and smoking, and if it could reliably predict OS. We performed univariate and multivariate Cox regression analyses on TCGA-derived LUAD datasets. Multivariate Cox regression was used to study independent prognostic factors based on the prognosis nomogram plot drawn in R.

2.5. Functional annotation

Gene ontology (GO) and Kyoto Encyclopedia of Genes and Genomes (KEGG) analyses were conducted to determine the biological activities of selected lncRNAs. The abundance of these DElncs in the two groups from the TCGA database was studied by constructing a heatmap. Heterogeneities in biological activities in the two risk groups were analyzed by GSEA (http://software.broadinstitute.org/gsea/index.jsp).

2.6. Somatic mutation analysis

Somatic variant data of LUAD cases were preserved in the mutation annotation format (MAF) and analyzed using maftools [17]. Tumor mutation burden (TMB) scores of all LUAD cases were determined to analyze their relationship with the risk score. We calculated the TMB score as follows: (total mutations/total covered bases) $\times 10^6$. The Kaplan–Meier analysis was conducted to study the application of TMB in predicting the prognosis of LUAD with R package [18,19].

2.7. Immunotherapy response and chemosensitivity prediction

We applied the pRRophetic R package to predict the chemosensitivity of both risk groups from the LUAD cohorts. Anti-tumor

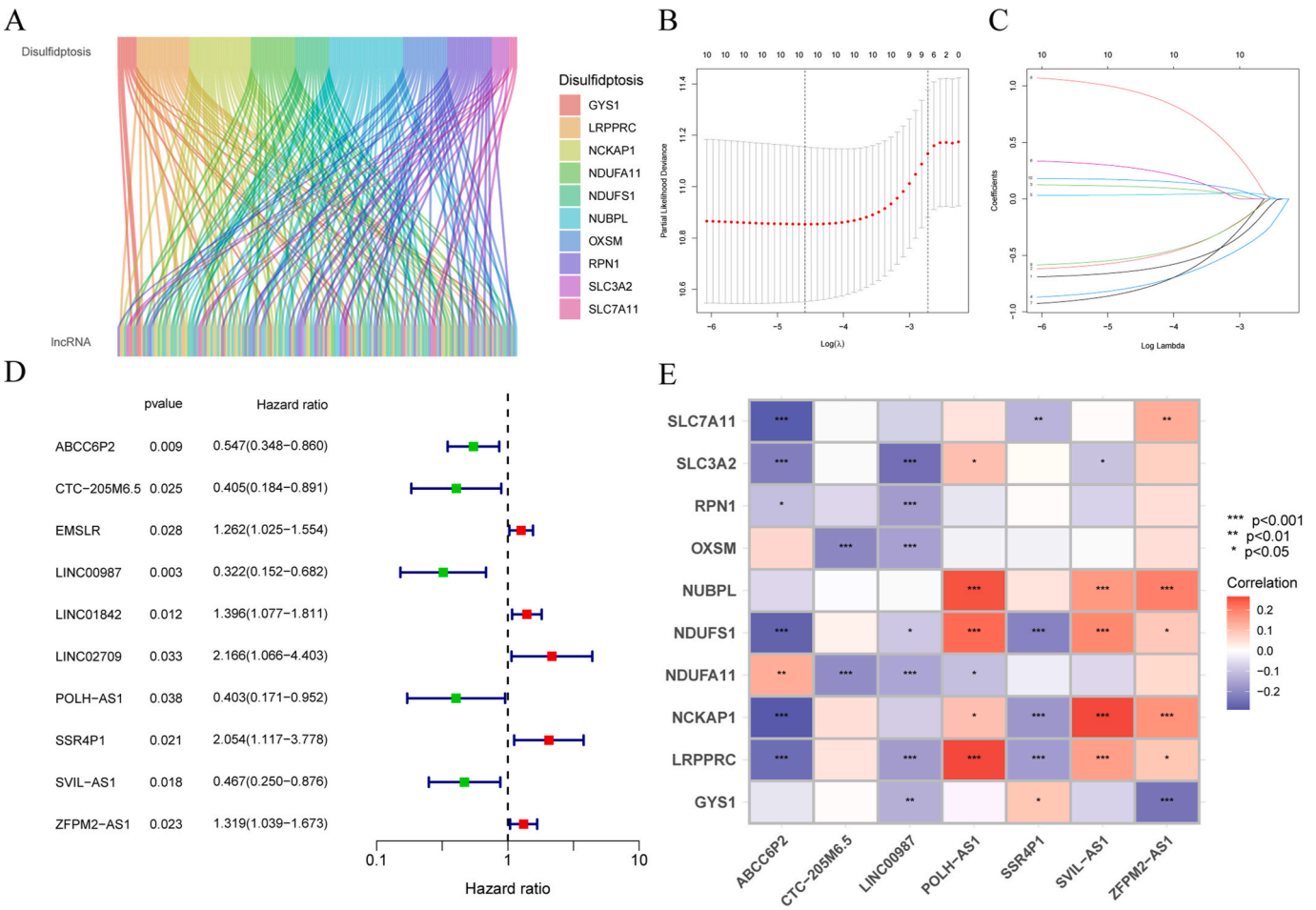

Fig. 1. Identification of disulfidptosis-related lncRNAs in The Cancer Genome Atlas cohort. (A) Sankey diagram of disulfidptosis-related lncRNAs. (B) LASSO coefficient profiles of disulfidptosis-related lncRNAs. (C) Partial likelihood deviance with change in the value of log(λ). (D) Forest plot of prognosis-related lncRNAs. (E) Heatmap showing the correlation between the 7 prognostic-related lncRNAs and 10 mRNAs.

therapeutics such as ABT-737, axitinib, AZD1208, BMS-754807, doramapimod, GSK269962A, JQ1, NU7741, PRT062607, ribociclib, SB216763, SB-505124, Tozasertib, and ZM447439 were frequently identified. Furthermore, their half-maximal inhibitory concentrations (IC_{50}) were analyzed [20]. In the computational framework, TIDE (http://tide.dfci.harvard.edu/) stands for tumor immune dysfunction and exclusion which can be used to assess tumor immune escape based on the gene expression in tumor tissues [21].

2.8. Reverse transcription-quantitative PCR (RT-qPCR)

A total of 26 LUAD samples were collected from the Affiliated Hospital of Qingdao University. The study was approved by the Ethics Committee of the Affiliated Hospital of Qingdao University. Primer sequences used are listed in Additional Table 2. Glyceraldehyde 3-phosphate dehydrogenase (GAPDH) was used as the endogenous reference in qPCR. The $2^{-\Delta\Delta Cq}$ approach was used to determine the relative expression of seven signature lncRNAs [22,23].

2.9. Statistical analysis

Different statistical methods were applied for data analysis. Log-rank tests and the Kaplan–Meier survival analysis were applied to determine the prognostic significance and compare patient survival among diverse subgroups of every dataset. Student's *t*-test was used to analyze normally distributed data, whereas the Wilcoxon test was applied to non-normally distributed data. The Kruskal–Wallis test was used as the non-parametric test for comparison among several groups. Spearman's correlation analysis was conducted to explore relationships between variables. $P < 0.05$ represented statistical significance.

3. Results

3.1. Disulfidptosis-related lncRNA detection

The literature reports 10 disulfidptosis-related lncRNAs (Table 1) [13]. We applied the mean expression >0.5 thresholds to obtain significant lncRNAs, excluding samples with low expression (Fig. 1A). Next relationships of the expression of disulfidptosis-related mRNAs and lncRNAs levels within LUAD samples were evaluated by limma package in R, with $P < 0.05$ and correlation coefficient >0.4 as thresholds. Finally, 93 disulfidptosis-related lncRNAs were obtained.

3.2. Prognostic disulfidptosis-related lncRNA model establishment and verification for TCGA cohort

In line with the LASSO Cox regression model, Fig. 1B displays the 10 most significant DElncs. In all, 10 OS-related disulfidptosis-related lncRNAs were acquired by distinctive formulas, following which risk scores of different samples were determined (Fig. 1C). The CIBERSORT analysis tool was used to study the intricate relationship between disulfidptosis-related genes and disulfidptosis-related lncRNAs levels. For instance, SLC3A2 and SLC7A11 were conversely related to ABCC6P2 (Fig. 1D), and seven lncRNAs were screened, whereas EMSLR,

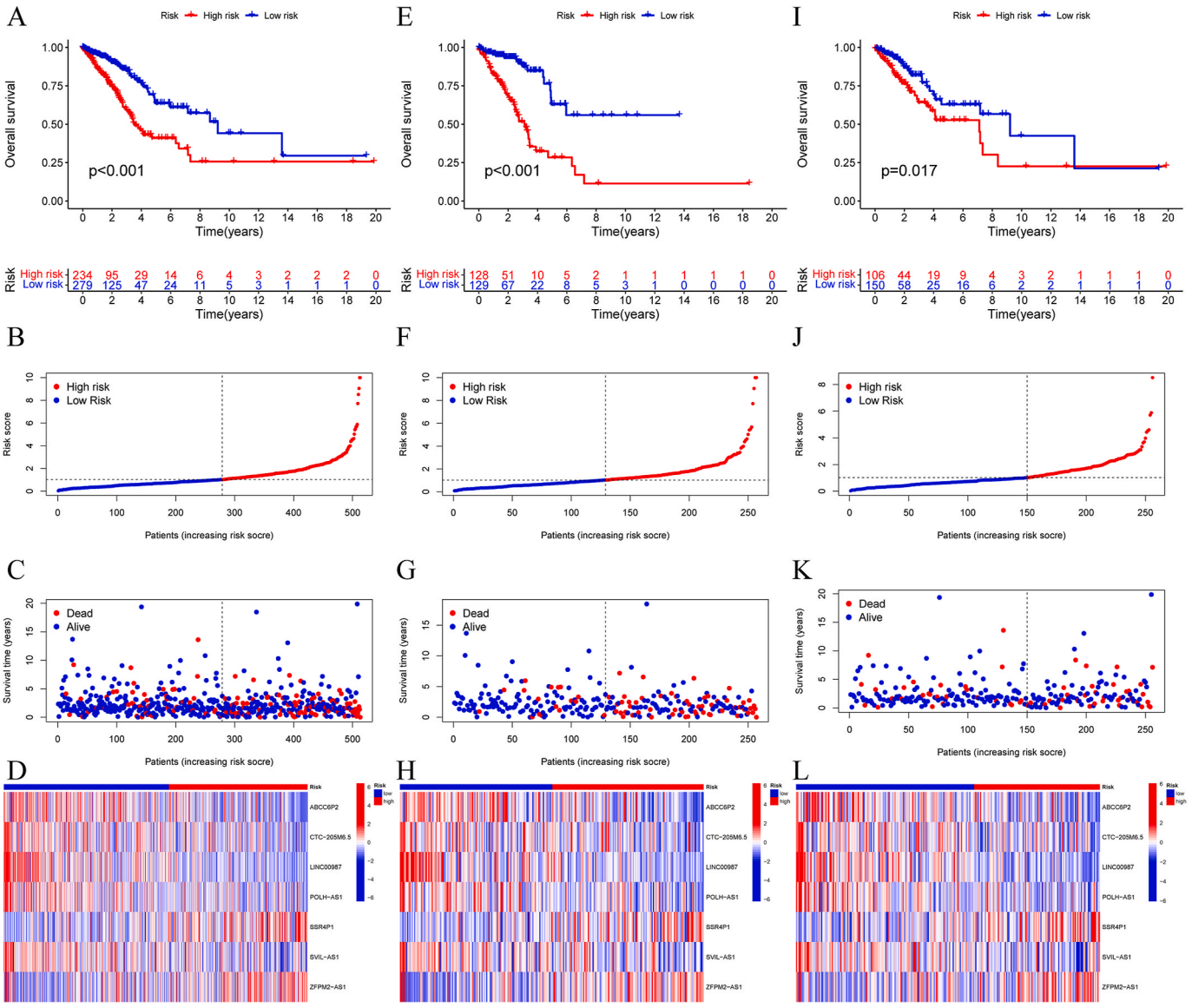

Fig. 2. Risk model for outcome prediction. (A, E, I) Kaplan–Meier curves for the overall survival of patients in the high- and low-risk groups in the TCGA-LUAD cohort, training cohort, and test cohort. (B, F, J) The distribution of risk scores for each patient in the TCGA-LUAD cohort, training cohort, and test cohort. (C, G, K) The distribution of overall survival status for every patient in the TCGA-LUAD cohort, training cohort, and test cohort. (D, H, L) Heatmap showing the expression of seven disulfidptosis-related lncRNAs in the TCGA-LUAD cohort, training cohort, and test cohort.

LincRNA01842, and LincRNA02709 were excluded due to insignificant correlation.

The median risk score was used to categorize 513 LUAD cases into high- ($n = 234$) and low-risk ($n = 279$) groups. Fig. 2A depicts that LUAD cases with high-risk scores had markedly increased mortality. The mortality risk increased with an elevation in the risk score, whereas the survival rate decreased (Fig. 2B and C). The risk heatmap displayed the expression patterns of lncRNAs between the two risk groups (Fig. 2D). The 513 TCGA-LUAD samples with sufficient data were randomized into training and validation cohorts; survival status along with heat map distribution of the training cohort is shown in Fig. 2E–H. Similar results were obtained for the validation cohort (Fig. 2I-L). The levels of seven disulfidptosis-related lncRNAs were markedly related to certain clinical factors, such as risk score and clinical stage in the univariate Cox hazard analysis and to age, clinical stage, tobacco, and risk score in multivariate Cox hazard analysis (Fig. 3A and B). The prognostic prediction model revealed significant differences in the expression of ABCC6P2, CTC-205M6.5, LINC00987, POLH-AS1, SSR4P1, SVIL-AS1, and ZFPM2-AS1.

3.3. Independent prognosis analysis of OS and predictive nomogram establishment in LUAD

Fig. 3C displays the 5-year survival rate. The area under the curve (AUC) values were calculated to compare the diagnostic efficiency of additional basic factors and risk scores among LUAD cases. For the 1-, 3-, and 5-year survival rates, the AUC values were 0.662, 0.71, and 0.659, respectively. Later, we analyzed if clinical factors such as age, gender, risk scores, smoking, and clinical stage independently predicted prognosis based on multivariate Cox regression along with the decision curve analysis. We found that risk score and clinical stage independently predicted OS (Fig. 3D). Moreover, the AUC values of the risk score and clinical stage models were 0.71 and 0.698, respectively. In addition, DCA was conducted to assess the clinical applicability of our prediction approach. The DCA results demonstrated that ROC achieved superior net benefits and a wide range of threshold probabilities in predicting patient survival (Fig. 3E). Moreover, our constructed nomogram resulted in superior benefits to the others signatures. The increased values relative to additional factors verified the better diagnostic efficiency of

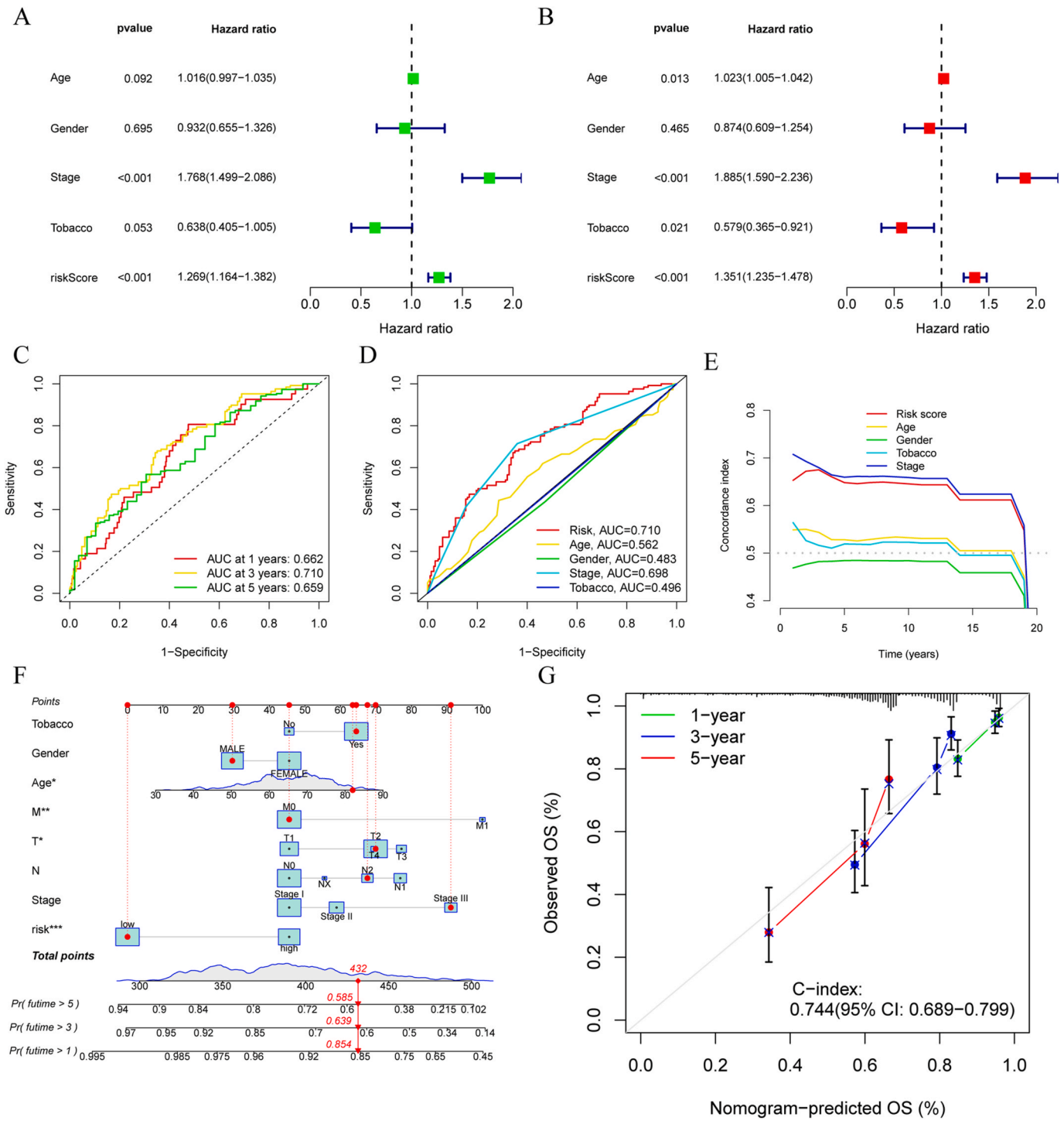

Fig. 3. Prognosis value of novel disulfidptosis-related lncRNA signatures. (A) Result of univariate Cox regression analysis. (B) Result of multivariate Cox regression analysis. (C) Accuracy of risk signature in predicting 1-, 3-, and 5-year ROC curves. (D) ROC curves of risk score and clinical characteristics. (E) Time-dependent C-index of the model compared with stage, age, gender for OS of patients with LUAD. (F) Nomogram uses a combination of clinicopathological variables and risk score to predict 1-, 3-, and 5-year overall survival. (G) Calibration curves for 1-, 3-, and 5-year overall survival.

our constructed disulfidptosis-related lncRNA signatures than the additional prognostic factors of LUAD cases. In addition, we built a nomogram to predict the OS in LUAD cases using independent factors obtained by a multivariate Cox risk regression model (Fig. 3F). The 1-, 3-, and 5-year calibration curves for our nomogram approached the standard curve, validating the favorable prediction performance of the model (Fig. 3G).

3.4. Construction of high risk score and survival with negative correlation in different clinical stages

The TCGA-LUAD cases were divided into high- and low-risk groups based on the risk scores. The prognosis analysis showed that high-risk cases had the poorest survival in clinical stages I and II (Fig. 4A). Thereafter, we pooled the data of additional clinical stages of LUAD cases and compared them between the two risk groups for prognosis (*p*

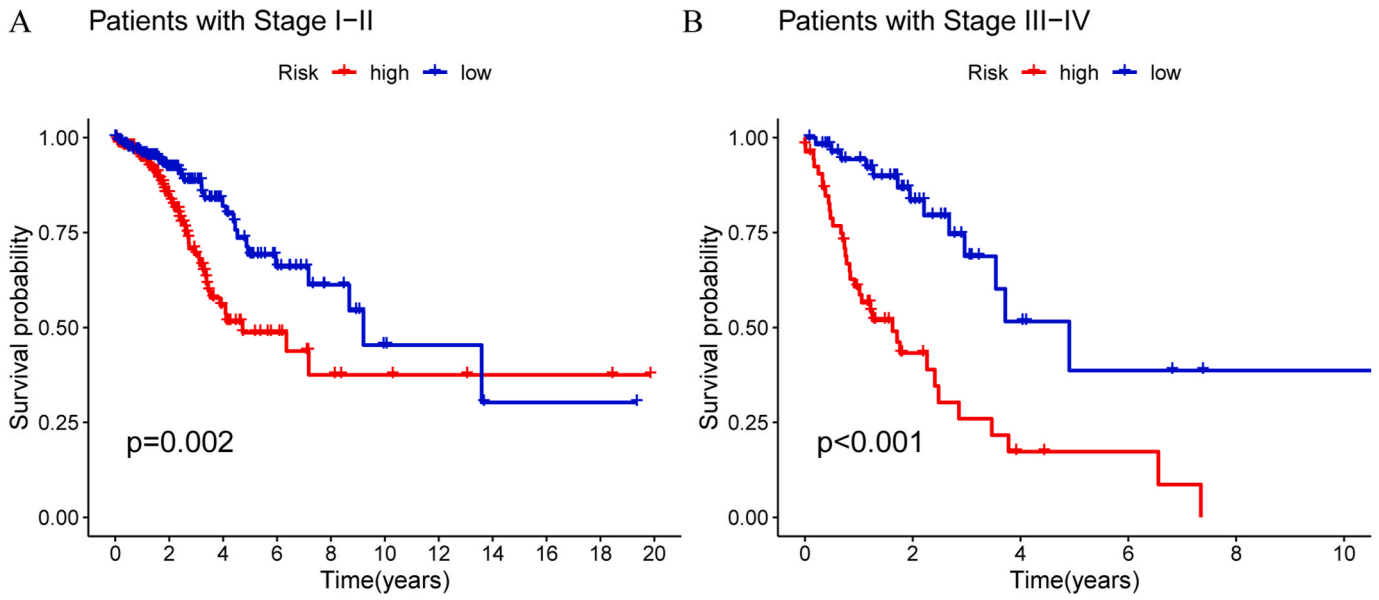

Fig. 4. Survival rates during different periods. (A, B) Mortality rate is higher in both early- and late-stage high-risk patients with LUAD.

< 0.001, Fig. 4B). Therefore, high-risk LUAD cases had poor prognostic outcomes.

3.5. Enrichment analysis of disulfidptosis-related lncRNA signature and PCA analysis

The scatterplot three-dimensional (3D) program was used to capture 3D images for PCA in training (Fig. 5A), validation (Fig. 5B), and total LUAD cohort sets (Fig. 5C). The cohort diagram-based GO annotation revealed significant differences in biological process (BP), molecular functions (MF), and cellular components (CC) in the two groups. Disulfidptosis-related lncRNAs were largely associated with the "aminoglycoside antibiotic metabolic process," "polyketide metabolic process," "doxorubicin metabolic process," "progesterone metabolic process," "quinone metabolic process," "glycoside metabolic process," "tertiary alcohol metabolic process," and "hormone metabolic process" (Fig. 5D and E). The bubble plot-based KEGG enrichment analysis revealed that disulfidptosis-related lncRNAs were primarily enriched in "steroid hormone biosynthesis," "arachidonic acid metabolism," "thyroid hormone synthesis," "bile secretion," "complement and coagulation cascades," "metabolism of xenobiotics by cytochrome P450," "folate biosynthesis," and "chemical carcinogenesis" (Fig. 5F). The GSEA in both risk groups was analyzed based on several GSEA diagrams using the screening criteria below: FDR <0.25 and NOM $P < 0.05$ (Fig. 5G and H). The five most significant functions related to the high-risk group included "oxidative phosphorylation," "steroid hormone biosynthesis," "Parkinson's disease," "pentose and glucuronate interconversions," and "ribosomes." In addition, the five most significant functions related to the low-risk group included "hematopoietic cell lineage," "cytokine receptor interaction," "primary immunodeficiency," and "intestinal immune network for IgA production."

3.6. TMB analysis and survival analysis of TMB

TME is previously suggested to be associated with LUAD distant metastases, drug sensitivity, and immunotherapeutic response [24–26]. Stromal and immune cell levels within TME can be represented by stromal score and immune score, respectively. We found that low-risk cases had increased proportions of stromal cells (Fig. 6A). Thereafter, we applied ssGSEA to investigate the infiltration levels of 16 immune cells and obtained scores of 13 immunological functions to assess the relationship of immune infiltration with risk mode. High-risk cases had increased T regulatory cells (Tregs), and heightened infiltration of macrophages M0, whereas low-risk cases showed increased infiltration of $CD4^+$ T memory resting cells and enhanced immunological functions such as those of DCs, B cells, $CD8^+$ T cells, T cell co-inhibitory molecules, and Th2 cells (Fig. 6B–D). The distribution of somatic mutation genes in both risk-score subgroups was analyzed. In Fig. 6E, cases showing high-risk scores exhibited a higher frequency of somatic mutations compared with low-risk scores counterparts. High-risk cases displayed higher TMB relative to low-risk counterparts (Fig. 6F). Subsequently, we pooled the data of H-TMB groups and compared them against the L-TMB group to analyze patient prognosis, with p-value $= 0.021$ (Fig. 6G). Later, LUAD cases were divided into four molecular subtype groups according to the TMB levels and risk scores, including TMB high + high risk, TMB high + low risk, TMB low + high risk, and TMB low + low risk. The prognosis analysis revealed that TMB high + high-risk cases showed the poorest survival than the remaining three groups (Fig. 6H). The effect of infiltration of tumor immune cells on gene levels in cancer samples was analyzed using the TIDE scores, which were used for predicting immune checkpoint blockade therapeutic responses. High-risk cases displayed an increased TIDE score (Fig. 6I).

3.7. Prognostic gene levels and drug sensitivity of cancer cells

We next evaluated whether lncRNA signatures could be applied to systemic treatments. The drug IC_{50} values were determined using the pRRophetic algorithm to predict the function of disulfidptosis-related lncRNAs in chemotherapeutic response in both risk groups. Thus, LUAD cases exhibited sensitivity to 14 conventional anti-tumor drugs (Fig. 7).

3.8. Validation of lncRNA prognostic signatures

We conducted qRT-PCR to evaluate the levels of seven prognostic disulfidptosis-related lncRNAs in A549 cells and compared them with those in healthy BEAS-2B lung cells. The qRT-PCR analysis demonstrated that the expression of *CTC-205M6.5*, *Linc00987*, *SSR4P1*, *SVIL-AS1*, and *ZFPM2-AS1* genes was remarkably elevated in A549 cells than in normal cells, whereas the expression of *ABCC6P2* and *POLH-AS1* genes showed an opposite trend (Fig. 8).

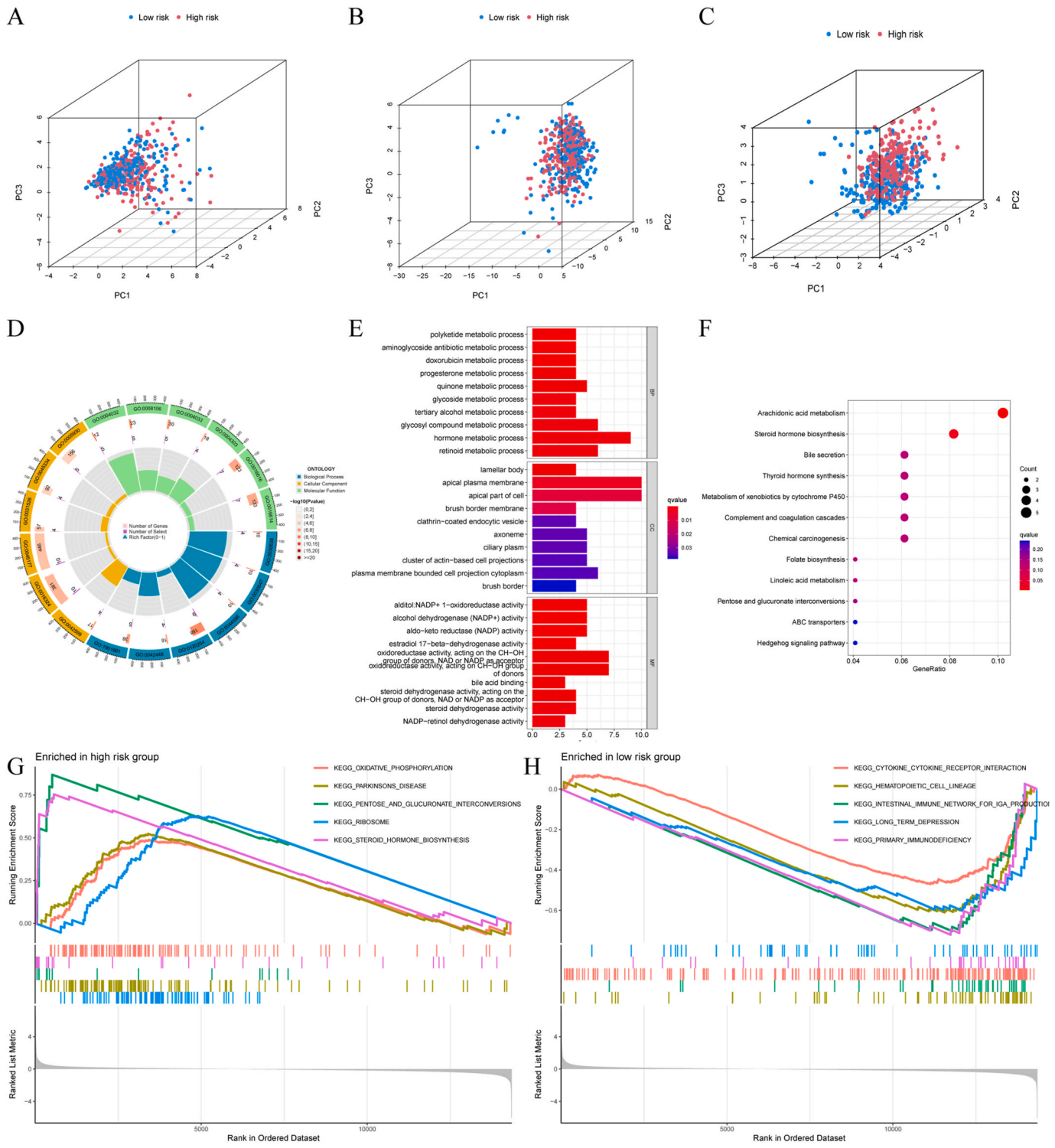

Fig. 5. Gene enrichment analysis. (A) PCA of disulfidptosis-related lncRNA expression in the training cohort. (B) PCA of disulfidptosis-related lncRNA expression in the test cohort. (C) PCA of disulfidptosis-related lncRNA gene expression in the TCGA-LUAD cohort. (D, E) GO enrichment analysis of disulfidptosis-related lncRNAs. (F) KEGG enrichment analysis of disulfidptosis-related lncRNAs. (G, H) KEGG pathway analysis for high- and low-risk LUAD patients.

4. Discussion

Among the different NSCLC subtypes, LUAD displays the highest prevalence. Although the clinical and scientific world has witnessed tremendous achievements in the screening, diagnosis, and treatment of LUAD, little is known about its pathogenic mechanism due to the associated complex molecular dynamics and genetics [27]. LncRNAs are non-coding gene biomarkers that have been implicated in tumorigenesis and cancer development, such as in LUAD [28,29]. However, information on disulfidptosis-related lncRNAs that can predict LUAD prognostic outcomes remains unclear. Therefore, we constructed a prognosis model by detecting disulfidptosis-related lncRNAs for predicting the OS of LUAD cases.

In total, 93 disulfidptosis-related lncRNAs were obtained through

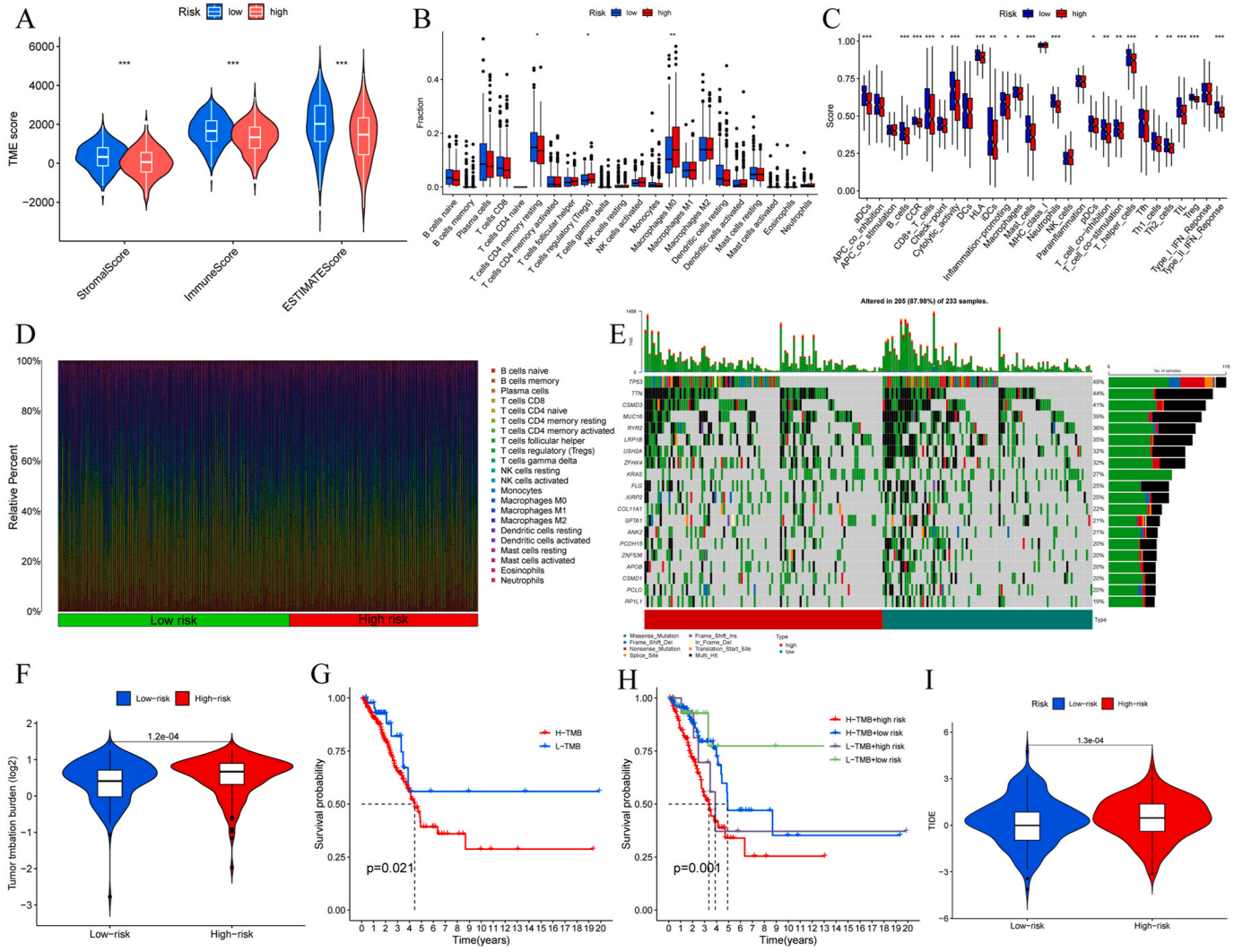

Fig. 6. Tumor immune microenvironment analysis and immunotherapy response. (A) The ESTIMATE, immune, and stromal scores for the tumor microenvironment of patients with LUAD in high- and low-risk groups. (B, C) The ssGSEA scores of immune cells and immune functions in the two risk groups. (D) Proportions of 22 tumor infiltrating immune cells in individual LUAD patients. (E) Waterfall plot of somatic mutation landscape of low- and high-risk groups. (F) TMB for different risk subgroups. (G) The Kaplan–Meier survival curve reveals the OS rate of patients in H-TMB and L-TMB groups. (H) The Kaplan–Meier survival curve shows the OS rate of patients in the H-TMB + high-risk, H-TMB + low-risk, L-TMB + high risk, and L-TMB + low risk groups. (I) Differences in TIDE score in high and low-risk groups.

correlation analysis. Univariate Cox regression analysis revealed 10 prognostic disulfidptosis-related lncRNAs for LUAD. Dimensionality reduction was completed with Lasso regression analysis to avoid overfitting. In addition, seven disulfidptosis-related lncRNA (showing the lowest Akaike Information Criterion [AIC] values)-based signatures were constructed using the multivariate Cox regression analysis. The LUAD cases were categorized into low- and high-risk groups according to their median risk scores. Using a combination of univariate and multivariate Cox regression analyses, the risk score was applied to independently predict LUAD prognosis. Later, AUCs were determined to verify the discrimination and accuracy of lncRNA signatures. Furthermore, the multivariate regression model was constructed to directly reflect the function of risk scores in OS prognosis.

ABCC6P2 has been previously suggested to affect the pseudoxanthoma elasticum phenotype [30]. Moreover, CTC-205M6 independently predicted the prognosis of clear cell renal cell carcinoma patients [31]. The reduced levels of lncRNA LINC00987 in LUAD predict poor prognosis and decreased immunotherapy response [32]. Emerging evidence has suggested that POLH-AS1 can be used as a prognostic and survival marker in patients with hepatocellular carcinoma [33,34]. SVIL-AS1 suppressed chemoresistance by sponging miR-103a while increasing the levels of ICE1, and it could be the possible anti-LUAD chemotherapeutic target [35]. Han et al. demonstrated that ZFPM2-AS1 promoted cell growth, migration, and epithelial-to-mesenchymal transition of LUAD cells [36]. However, the effects of lncRNA SSR4P1 are unclear. Consequently, more research on these lncRNAs is warranted to develop new strategies to diagnose and treat LUAD.

Tumor-associated immune response exerts a critical effect on cell migration and infiltration within TME. Disulfidptosis and lncRNAs are important regulatory factors and components of tumor-associated immune responses [37,38]. Our immune-related GSEA results revealed that metabolic pathways and immune system processes were mostly related to low-risk groups relative to the high-risk counterparts, thereby indicating that the low-risk groups displayed disulfidptosis-related anticancer immunity, finally promoting LUAD survival.

The functions of lncRNAs have been increasingly discovered in recent years, with their functions being studied in disulfidptosis in anticancer treatment. However, the relationships of lncRNAs with disulfidptosis should be further analyzed, in particular in LUAD. In the present work, we obtained 10 ferroptosis-related lncRNAs from TCGA. We next analyzed the functions of these lncRNAs within metabolic

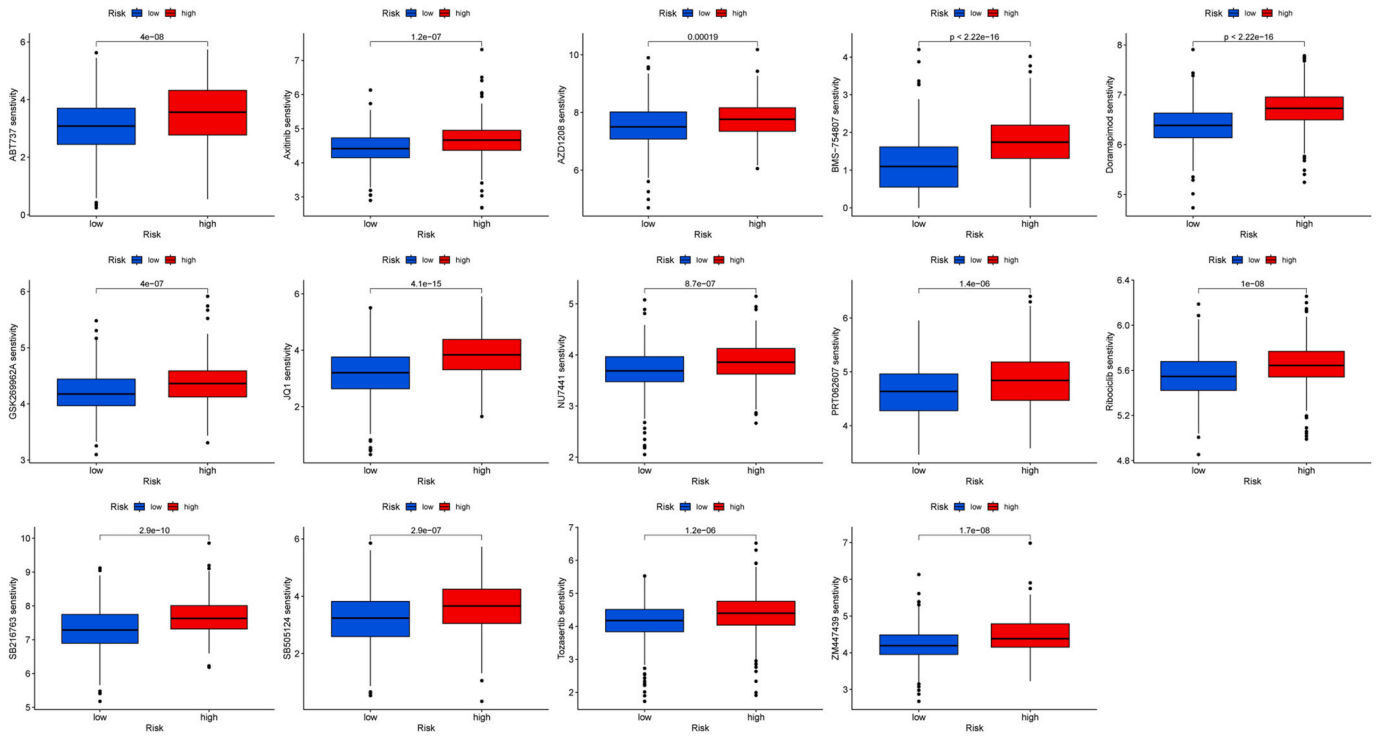

Fig. 7. Prediction of response to common chemotherapeutic drugs between low- and high-risk groups. Patients in the high-risk group ($n = 267$) showed higher estimated half-maximal inhibitory concentration relative to patients in the low-risk group ($n = 244$).

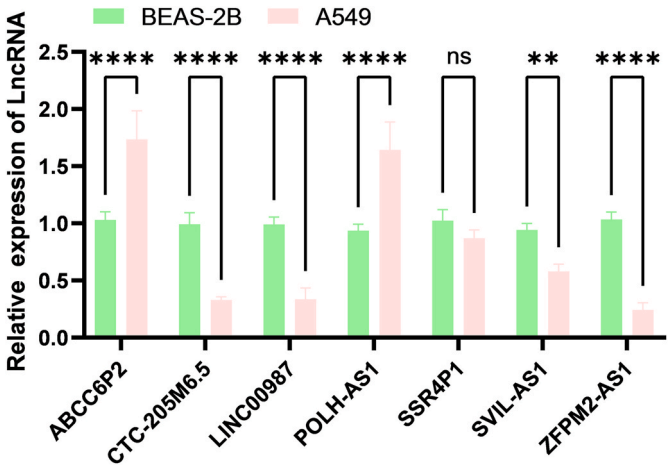

Fig. 8. Expression of ferroptosis-related long non-coding RNAs in lung adenocarcinoma tissues by reverse transcription-quantitative PCR. $^*P < 0.05$.

pathways and immune responses.

Our study had certain limitations. First, we only obtained TCGA-derived data to construct the disulfidptosis-related lncRNA prognosis model and verify it. In addition, only a few experiments were conducted to detect the expression of detected disulfidptosis-related lncRNAs within clinical cells and tissues. Consequently, more *in vitro* experiments are warranted to elucidate the mechanisms underlying the functions of disulfidptosis-related lncRNAs in LUAD.

5. Conclusion

Six prognostic disulfidptosis-related lncRNAs related to immune responses in LUAD were detected and verified. The findings demonstrated lncRNAs as possible prognostic biomarkers and novel treatment strategies targeting ferroptosis, which can improve the prognosis of patients with LUAD.

Ethics approval and consent to participate

The study was approved by the Ethics Committee of the Affiliated Hospital of Qingdao University.

Consent for publication

Not applicable.

Availability of data and materials

The datasets analyzed for this study can be found on the TCGA-LUAD project (http://www.cancer.gov/tcga). Original data referenced in the study are included in the article/supplementary materials, and further inquiries can be directed to the corresponding author.

Funding

The present study was supported by the National Key Research and Development Program (2019YFE0120100), the National Natural Science Foundation of Shandong (ZR202103040278), and Health Development Promotion Project (BJHA-CRP-094).

CRediT authorship contribution statement

Shifeng Liu: Writing – original draft, Visualization, Validation, Supervision, Software, Resources, Project administration, Methodology, Investigation, Funding acquisition, Formal analysis, Data curation, Conceptualization. **Song Wang:** Conceptualization. **Jian Guo:** Data curation. **Congxiao Wang:** Formal analysis. **Hao Zhang:** Funding acquisition. **Dongliang Lin:** Investigation. **Yuanyong Wang:** Writing – review & editing. **Xiaokun Hu:** Writing – review & editing, Software, Resources.

Declaration of competing interest

The authors declare that they have no known competing financial interests or personal relationships that could have appeared to influence the work reported in this paper.

Acknowledgements

Not applicable.

Appendix A. Supplementary data

Supplementary data to this article can be found online at https://doi.org/10.1016/j.ncrna.2024.03.006.

References

[1] R.L. Siegel, K.D. Miller, N.S. Wagle, A. Jemal, Cancer statistics, 2023, CA A Cancer J. Clin. 73 (1) (2023) 17–48, https://doi.org/10.3322/caac.21763. PMID: 36633525.
[2] S.J. Adams, E. Stone, D.R. Baldwin, R. Vliegenthart, P. Lee, F.J. Fintelmann, Lung cancer screening, Lancet 401 (10374) (2023) 390–408, https://doi.org/10.1016/S0140-6736(22)01694-4. PMID: 36563698.
[3] Y. Wang, Z. Wang, C. Shao, G. Lu, M. Xie, J. Wang, et al., Melatonin may suppress lung adenocarcinoma progression via regulation of the circular noncoding RNA hsa_circ_0017109/miR-135b-3p/TOX3 axis, Published Online First: 2022/06/07, J. Pineal Res. (2022) e12813, https://doi.org/10.1111/jpi.12813. PMID: 35661247.
[4] Y. Wang, G. Lu, X. Xue, M. Xie, Z. Wang, Z. Ma, et al., Characterization and validation of a ferroptosis-related LncRNA signature as a novel prognostic model for lung adenocarcinoma in tumor microenvironment, Front. Immunol. 13 (2022) 903758, https://doi.org/10.3389/fimmu.2022.903758. PMID: 36016939.
[5] T.V. Denisenko, I.N. Budkevich, B. Zhivotovsky, Cell death-based treatment of lung adenocarcinoma, Cell Death Dis. 9 (2) (2018) 117, https://doi.org/10.1038/s41419-017-0063-y. PMID: 29371589.
[6] C. Nossing, K.M. Ryan, 50 years on and still very much alive: 'Apoptosis: a basic biological phenomenon with wide-ranging implications in tissue kinetics', Br. J. Cancer 128 (3) (2023) 426–431, https://doi.org/10.1038/s41416-022-02020-0. PMID: 36369364.
[7] E. Koren, Y. Fuchs, Modes of regulated cell death in cancer, Cancer Discov. 11 (2) (2021) 245–265, https://doi.org/10.1158/2159-8290.CD-20-0789. PMID: 33462123.
[8] L. Galluzzi, I. Vitale, S.A. Aaronson, J.M. Abrams, D. Adam, P. Agostinis, et al., Molecular mechanisms of cell death: recommendations of the nomenclature committee on cell death 2018, Cell Death Differ. 25 (3) (2018) 486–541, https://doi.org/10.1038/s41418-017-0012-4. PMID: 29362479.
[9] D. Tang, R. Kang, T.V. Berghe, P. Vandenabeele, G. Kroemer, The molecular machinery of regulated cell death, Cell Res. 29 (5) (2019) 347–364, https://doi.org/10.1038/s41422-019-0164-5. PMID: 30948788.
[10] B.A. Carneiro, W.S. El-Deiry, Targeting apoptosis in cancer therapy, Nat. Rev. Clin. Oncol. 17 (7) (2020) 395–417, https://doi.org/10.1038/s41571-020-0341-y. PMID: 32203277.
[11] X. Feng, Q. Song, A. Yu, H. Tang, Z. Peng, X. Wang, Receptor-interacting protein kinase 3 is a predictor of survival and plays a tumor suppressive role in colorectal cancer, Neoplasma 62 (4) (2015) 592–601, https://doi.org/10.4149/neo_2015_071. PMID: 25997957.
[12] A.D. Garg, P. Agostinis, Cell death and immunity in cancer: from danger signals to mimicry of pathogen defense responses, Immunol. Rev. 280 (1) (2017) 126–148, https://doi.org/10.1111/imr.12574. PMID: 29027218.
[13] X. Liu, L. Nie, Y. Zhang, Y. Yan, C. Wang, M. Colic, et al., Actin cytoskeleton vulnerability to disulfide stress mediates disulfidptosis, Nat. Cell Biol. 25 (3) (2023) 404–414, https://doi.org/10.1038/s41556-023-01091-2. PMID: 36747082.
[14] M. Yuan, Y. Wang, Q. Sun, S. Liu, S. Xian, F. Dai, et al., Identification of a nine immune-related lncRNA signature as a novel diagnostic biomarker for hepatocellular carcinoma, BioMed Res. Int. 2021 (2021) 9798231, https://doi.org/10.1155/2021/9798231. PMID: 33506049.
[15] D. Zhou, X. Liu, X. Wang, F. Yan, P. Wang, H. Yan, et al., A prognostic nomogram based on LASSO Cox regression in patients with alpha-fetoprotein-negative hepatocellular carcinoma following non-surgical therapy, BMC Cancer 21 (1) (2021) 246, https://doi.org/10.1186/s12885-021-07916-3. PMID: 33685417.
[16] Y. Lai, Y. Wang, Y. Wu, M. Wu, S. Xing, Y. Xie, et al., Identification and validation of serum CST1 as a diagnostic marker for differentiating early-stage non-small cell lung cancer from pulmonary benign nodules, Cancer Control 29 (2022) 10732748221104661, https://doi.org/10.1177/10732748221104661. PMID: 35653624.
[17] A. Mayakonda, D.C. Lin, Y. Assenov, C. Plass, H.P. Koeffler, Maftools: efficient and comprehensive analysis of somatic variants in cancer, Genome Res. 28 (11) (2018) 1747–1756, https://doi.org/10.1101/gr.239244.118. PMID: 30341162.
[18] D.R. Robinson, Y.M. Wu, R.J. Lonigro, P. Vats, E. Cobain, J. Everett, et al., Integrative clinical genomics of metastatic cancer, Nature 548 (7667) (2017) 297–303, https://doi.org/10.1038/nature23306. PMID: 28783718.
[19] S. Zhao, W. Ji, Y. Shen, Y. Fan, H. Huang, J. Huang, et al., Expression of hub genes of endothelial cells in glioblastoma-A prognostic model for GBM patients integrating single-cell RNA sequencing and bulk RNA sequencing, BMC Cancer 22 (1) (2022) 1274, https://doi.org/10.1186/s12885-022-10305-z. PMID: 36474171.
[20] P. Geeleher, N.J. Cox, R.S. Huang, Clinical drug response can be predicted using baseline gene expression levels and in vitro drug sensitivity in cell lines, Genome Biol. 15 (3) (2014) R47, https://doi.org/10.1186/gb-2014-15-3-r47. PMID: 24580837.
[21] H. Chi, G. Peng, J. Yang, J. Zhang, G. Song, X. Xie, et al., Machine learning to construct sphingolipid metabolism genes signature to characterize the immune landscape and prognosis of patients with uveal melanoma, Front. Endocrinol. 13 (2022) 1056310, https://doi.org/10.3389/fendo.2022.1056310. PMID: 36568076.
[22] Y. Wang, R. Xu, D. Zhang, T. Lu, W. Yu, Y. Wo, et al., Circ-ZKSCAN1 regulates FAM83A expression and inactivates MAPK signaling by targeting miR-330-5p to promote non-small cell lung cancer progression, Transl. Lung Cancer Res. 8 (6) (2019) 862–875, https://doi.org/10.21037/tlcr.2019.11.04. PMID: 32010565.
[23] Y. Shi, Y. Zhao, Y. Wang, An inflammatory response-related gene signature can predict the prognosis and impact the immune status of lung adenocarcinoma, Cancers 14 (23) (2022), https://doi.org/10.3390/cancers14235744. PMID: 36497225.
[24] E.S.D. Dias, G.B. Borba, J.R. Beal, G. Botrus, A. Osawa, S.E.A. Araujo, et al., Response to abemaciclib and immunotherapy rechallenge with nivolumab and ipilimumab in a heavily pretreated TMB-H metastatic squamous cell lung cancer with CDKN2A mutation, PIK3CA amplification and TPS 80%: a case report, Int. J. Mol. Sci. 24 (4) (2023), https://doi.org/10.3390/ijms24044209. PMID: 36835617.
[25] B. Ricciuti, M.M. Awad, Atezolizumab plus bevacizumab in TMB-high non-small cell lung cancers-the hunt for predictive biomarkers to optimize treatment selection, JAMA Oncol. 9 (3) (2023) 353–354, https://doi.org/10.1001/jamaoncol.2022.5801. PMID: 36520420.
[26] Q. Han, S. Liu, Z. Cui, Q. Wang, T. Ma, L. Jiang, et al., Case report and literature review: diagnosis, tailored genetic counseling and cancer prevention for a locally advanced dMMR/MSI-H/TMB-H lung cancer patient with concurrent lynch syndrome mediated by a rare PMS2 splicing variant (c.1144+1G>A), Front. Genet. 12 (2021) 799807, https://doi.org/10.3389/fgene.2021.799807. PMID: 35116055.
[27] Y. Wang, T. Lu, Y. Wo, X. Sun, S. Li, S. Miao, et al., Identification of a putative competitive endogenous RNA network for lung adenocarcinoma using TCGA datasets, PeerJ 7 (2019) e6809, https://doi.org/10.7717/peerj.6809. PMID: 31065463.
[28] W. Ren, Y. Yuan, X. Chen, H. Zhai, Y. An, L. Tang, et al., Identification and validation of long non-coding RNA LCIIAR as a biomarker in LUAD, Front. Oncol. 12 (2022) 933071, https://doi.org/10.3389/fonc.2022.933071. PMID: 35860557.
[29] Y. Liu, L. Liang, L. Ji, F. Zhang, D. Chen, S. Duan, et al., Potentiated lung adenocarcinoma (LUAD) cell growth, migration and invasion by lncRNA DARS-AS1 via miR-188-5p/KLF12 axis, Aging (Albany NY) 13 (19) (2021) 23376–23392, https://doi.org/10.18632/aging.203632. PMID: 34644678.
[30] M.K. Kringen, C. Stormo, J.P. Berg, S.F. Terry, C.M. Vocke, S. Rizvi, et al., Copy number variation in the ATP-binding cassette transporter ABCC6 gene and ABCC6 pseudogenes in patients with pseudoxanthoma elasticum, Mol Genet Genomic Med 3 (3) (2015) 233–237, https://doi.org/10.1002/mgg3.137. PMID: 26029710.
[31] D. Shi, Q. Qu, Q. Chang, Y. Wang, Y. Gui, D. Dong, A five-long non-coding RNA signature to improve prognosis prediction of clear cell renal cell carcinoma, Oncotarget 8 (35) (2017) 58699–58708, https://doi.org/10.18632/oncotarget.17506. PMID: 28938589.
[32] J. Ma, X. Lin, X. Wang, Q. Min, T. Wang, C. Tang, Reconstruction and analysis of the immune-related LINC00987/A2M Axis in lung adenocarcinoma, Front. Mol. Biosci. 8 (2021) 644557, https://doi.org/10.3389/fmolb.2021.644557. PMID: 33987201.
[33] Z. Zhang, W. Gao, X. Tan, T. Deng, W. Zhou, H. Jian, et al., Construction and verification of a novel circadian clock related long non-coding RNA model and prediction of treatment for survival prognosis in patients with hepatocellular carcinoma, BMC Cancer 23 (1) (2023) 57, https://doi.org/10.1186/s12885-023-10508-y. PMID: 36647032.
[34] X. Lin, S. Yang, A prognostic signature based on the expression profile of the ferroptosis-related long non-coding RNAs in hepatocellular carcinoma, Adv. Clin. Exp. Med. 31 (10) (2022) 1099–1109, https://doi.org/10.17219/acem/149566. PMID: 35581934.
[35] L. Guo, L. Ding, J. Tang, Identification of a competing endogenous RNA axis "SVIL-AS1/miR-103a/ICE1" associated with chemoresistance in lung adenocarcinoma by comprehensive bioinformatics analysis, Cancer Med. 10 (17) (2021) 6022–6034, https://doi.org/10.1002/cam4.4132. PMID: 34264003.
[36] S. Han, D. Cao, J. Sha, X. Zhu, D. Chen, LncRNA ZFPM2-AS1 promotes lung adenocarcinoma progression by interacting with UPF1 to destabilize ZFPM2, Mol. Oncol. 14 (5) (2020) 1074–1088, https://doi.org/10.1002/1878-0261.12631. PMID: 31919993.
[37] P. Zheng, C. Zhou, Y. Ding, S. Duan, Disulfidptosis: a new target for metabolic cancer therapy, J. Exp. Clin. Cancer Res. 42 (1) (2023) 103, https://doi.org/10.1186/s13046-023-02675-4. PMID: 37101248.
[38] C. Qi, J. Ma, J. Sun, X. Wu, J. Ding, The role of molecular subtypes and immune infiltration characteristics based on disulfidptosis-associated genes in lung adenocarcinoma, Aging (Albany NY) 15 (11) (2023) 5075–5095, https://doi.org/10.18632/aging.204782. PMID: 37315289.